Monitoring Space Weather with a Sensitive 1 U CubeSat Mass Spectrometer

Rico G. Fausch
University of Bern, Physics Institute
Sidlerstrasse 5
3012 Bern
rico.fausch@unibe.ch

Claudio Zimmermann
University of Bern, Physics Institute
Sidlerstrasse 5
3012 Bern
claudio.zimmermann@unibe.ch

Thomas Gerber
University of Bern, Physics Institute
Sidlerstrasse 5
3012 Bern
thomas.gerber@unibe.ch

Janis Schertenleib
University of Bern, Physics Institute
Sidlerstrasse 5
3012 Bern
janis.schertenleib@unibe.ch

Martina Föhn
University of Bern, Physics Institute
Sidlerstrasse 5
3012 Bern
martina.foehn@unibe.ch

Audrey E. Aebi
University of Bern, Physics Institute
Sidlerstrasse 5
3012 Bern
audrey.aebi@unibe.ch

Peter Wurz
University of Bern, Physics Institute
Sidlerstrasse 5
3012 Bern
peter.wurz@unibe.ch

2023 IEEE Aerospace Conference | 978-1-6654-9032-0/23/$31.00 ©2023 IEEE | DOI: 10.1109/AERO55745.2023.10115572

***Abstract*—The chemical composition of Earth's upper atmosphere provides key insights into the status and evolution of the space weather. Earth's exosphere extends from hundreds of kilometers to ten thousands of kilometers. Characteristic measures of the exosphere include the altitude of the exobase, where the transition between the two flow regimes namely continuum flow and free-molecular flow occurs, the number density of species at given altitudes and their dynamics. The chemical composition can be measured, and the vertical structure can be converted into exospheric temperatures for each compound. Although major species dominate, the abundance of minor species, radicals and even traces of species might be underestimated, as they might represent more sensitive tracers of both the space weather influence on the atmosphere and the pollution of the outer atmosphere by decomposing space debris. Considering the complex sequence of chemical reactions, detailed mass spectrometric investigations are necessary. Despite some chemical species being measured during the latest measurements in the 1980s, the abundances of minor components, radicals and trace gasses remain unassessed until today, as previous instrumentation lacked both sensitivity and mass range. As these measures are of dynamic nature, constant monitoring with sensitive instrumentation and high cadence is demanded to derive data for meaningful investigations of the atmosphere composition in response to the exogenous and anthropogenic drivers. Here we report on the development of a novel mass spectrometer that provides sensitive in situ measurements of both the neutral gas and ions in Earth's upper atmosphere. The time-of-flight ion-optical system together with its detector provides a sensitivity that is comparable to full-scale mass spectrometers on board major deep space missions. In addition, this mass spectrometer directly measures species without contact with a wall, preventing on one hand complex species from hypervelocity impact induced bond-dissociation and on the other hand radicals from recombining before measuring at the usual orbital velocities exceeding 7 km/s. These unique instrument capabilities together with its performance empowers the instrument to measure the exosphere close to the exobase to determine scale heights of species reliably, identify and quantify the drivers of the exosphere, and derive almost real-time exospheric temperatures from the exosphere. Thanks to its size of 1 U, establishing a network consisting of several satellites for real-time space weather monitoring and its related forecasting becomes feasible, soon.**

TABLE OF CONTENTS

1. INTRODUCTION 1
2. INSTRUMENT DESIGN 3
3. ELECTRONICS 3
4. TEST FACILITIES...7
5. CONCLUSION 8
LIST OF ABBREVIATIONS, ACRONYMS AND SYMBOLS 8
ACKNOWLEDGEMENTS 9
REFERENCES 9
BIOGRAPHY 10

1. INTRODUCTION

In situ chemical composition measurements of neutral gas and ions are essential for understanding Earth's upper

978-1-6654-9032-0/23/$31.00 ©2023 IEEE

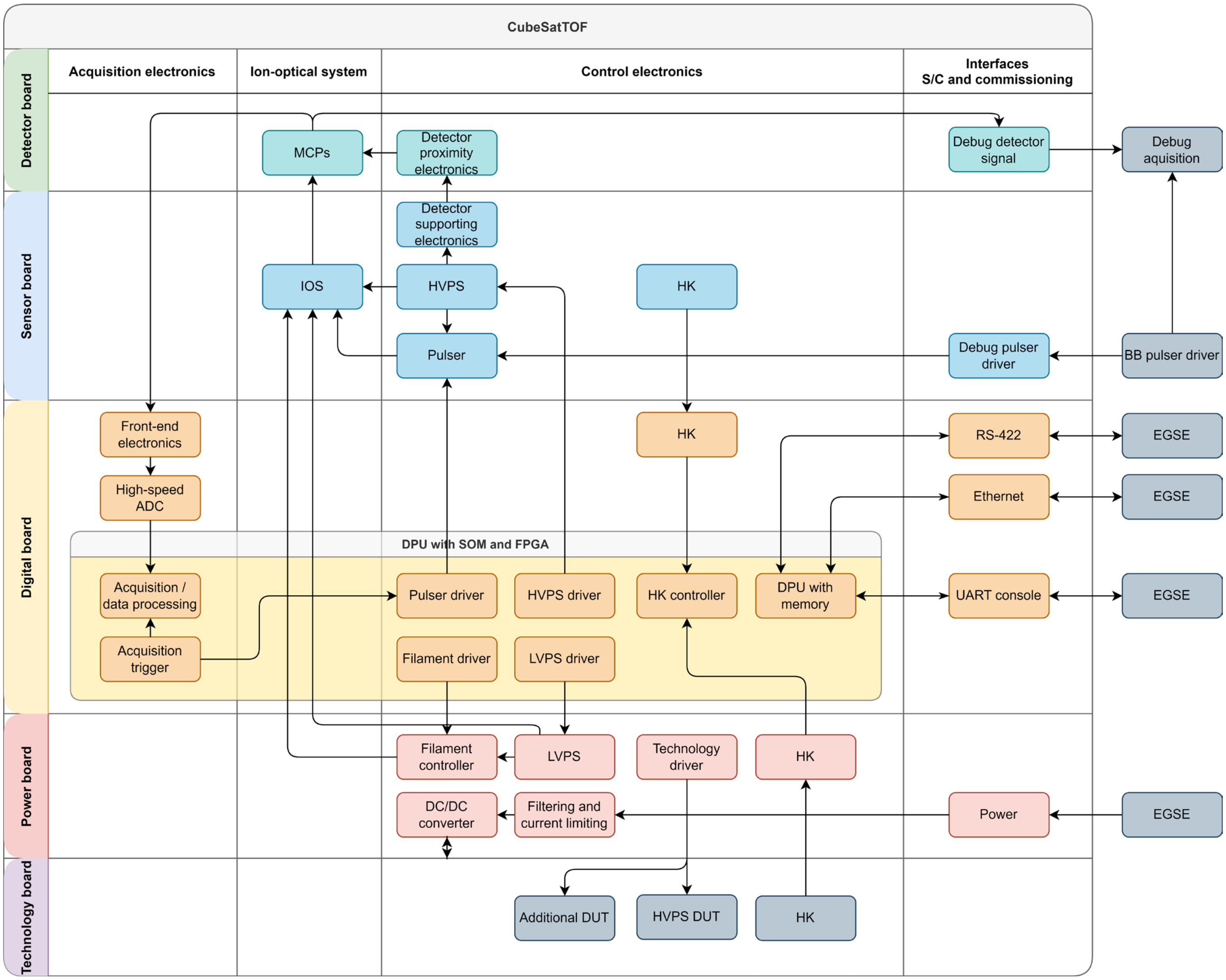

Figure 1. Block diagram of the CubeSatTOF instrument. Abbreviations are described in the text.

atmosphere and its responses to both exogenous and endogenous forcing. Especially measurements of the lower exosphere and thermosphere with mass spectrometers are necessary, as identified by recent reviews [1]–[5]. These reviews discuss the necessity of measuring the chemical composition of neutral species and ions and underline that no successful measurement with a mass spectrometer has been performed since the 1980s [6]. The limited sensitivity in combination with the upper limit of the mass range of about *m/z* 50 of these measurements was sufficient to detect the major species in the upper atmosphere (H, N, O, N_2, CO, O_2, Ar; H^+, He^+, N^+, O^+, N_2^+). The interest in this region is also reflected by the intention of NASA's Science Mission Directorate to release an announcement of opportunity for the Dynamical Neutral Atmosphere-Ionosphere Coupling (DYNAMIC) mission, soon [7].

The upper atmosphere is a dynamic region and includes the thermosphere, the exosphere, and the ionosphere (see reference [8], for example). The exosphere extends from some 400 km to thousands of kilometers, depending on the conditions (and models) [9]. The exosphere couples to the thermosphere, and the exobase separates them [10]. In the exosphere, ballistic trajectories determine the motion of species, as it is the case in an almost collision-free region. In the thermosphere, mixing dominates the trajectories resulting in a statistical motion. In addition, the ionosphere is embedded into this region as well. Species occasionally change their charge, i.e., from neutral to charged, and vice-versa by, for example, charge exchange processes. Hence, the exosphere serves as both source and sink for the ionosphere. However, although these ionization and recombination mechanisms are thought to be identified, their extent remains unclear. Moreover, even the precise altitude of the exobase is subject of debates. This lack of knowledge prevents concluding the influence of forcing on the upper atmosphere, i.e., understanding of the influence of space weather on Earth's atmosphere.

Hence, the constellation of high-performance exosphere science satellites (CHESS) mission was conceived to analyze the dynamics of both the chemical composition and number densities of species in the upper atmosphere [11]. The CHESS mission carries a global navigation satellite system

(GNSS) instrument for the analysis of the total number density and a complementary mass spectrometer for analyzing the chemical composition of species, their altitude profiles, and their variation in both space and time.

2. Instrument Design

Here we present a novel, miniaturized mass spectrometer that provides sensitive in situ measurements of both the neutral gas and ions in Earth's upper atmosphere enabled by its compact and powerful electronics. The instrument is a time-of-flight (TOF) mass spectrometer [12], referred to as CubeSatTOF, that fits into 1 U of a CubeSat and weighs 1 kg including shielding.

References [11], [13], [14] describe the design of the ion-optical system (IOS) and its application in detail. In brief, CubeSatTOF employs a novel ion-optical system referred to as the direct open source [13]. Present instruments used so far implemented either a closed or an open ion source. In a closed source, neutral particles are thermalized in an antechamber via multiple collisions with the chamber wall. In an open source, species are directly ionized and electrostatically deflected into the ion-optical system of the mass analyzer. In contrast, in the direct open source, neutral particles are not thermalized and ions are not deflected before entering the mass analyzer.

This novel technique avoids both hypervelocity impact induced bond-dissociation experienced in the closed source and the requirement of very high voltages to deflect a beam of high velocity ions in classical open source systems. While avoiding high voltages reduces complexity in engineering, avoiding hypervelocity impact induced bond-dissociation considerably simplifies the interpretation of the scientific data. At typical low Earth orbit (LEO) velocities of about 7.6 km/s, referred to as hypervelocity, incoming species have a kinetic energy about 0.3 eV for *m/z* 1, which scales linear with mass. For reference, the bond-dissociation energy of a carbon–carbon bond is 3.6 eV [15]. Thus, the collisions of incoming species with the wall of the antechamber typically fragment species. In addition, reactive species such as O and O_3 typically recombine with other species or fragments thereof in the antechamber before the mass analyzer records them. Inferring the original molecules from measurements of partially atomized species is already challenging for simple molecules in a mixture, and almost impossible for more complex species. Thus, measuring with this novel gas inlet system enables reliable measurements of both reactive and non-atomic species.

The direct open source is capable of measuring neutral species and positively charged ions. At the entrance of the instrument, a robust thermionic emitter provides electron ionization at about 70 eV for ionizing incoming neutral species. To measure local ions, the filament is turned off. A high voltage pulser extracts the species from the ion source representing the start signal for the TOF of the incoming species. Electrostatic lenses focus the ion beam into a field-free drift section providing mass separation. A grid-free ion mirror (reflectron) [16], [17] compensates for variations in initial energy. It also increases the flight path, as another drift section precedes the ions' impact on the multi-channel plate (MCP) detector, representing the stop signal. The MCPs amplify the impacts by about a factor of 10^6 allowing for single ion analysis on a routinely basis [18], [19]. The recorded signal is then easily converted into a mass spectrum (see reference [20], for example). The ion-optical system and electronics are designed to analyze a full mass spectrum of the mass range *m/z* 1 to 200 simultaneously with a repetition frequency of nominally 10 kHz (up to 40 kHz in extended mode). The data processing unit operating the electronic front-end histograms the recorded waveforms to output a full mass spectrum every 100 ms to 10 s translating to a spatial resolution of less than 1 km in LEO.

CubeSatTOF achieves mass resolutions exceeding $m/\Delta m$ 200, where Δm is the full width at half maximum (FWHM) of mass peak m. This mass resolution allows for clearly resolving isotopes of lower and higher masses, and outperforms comparable instrumentation concepts by an order of magnitude [21], [22]. The transmission of the ion-optical system of 100 %, as demonstrated by SIMION simulations [13], ensures a high sensitivity enabling analysis of even traces of species. In addition, it prevents mass fractionation, as a limited transmission may be mass dependent, hence ensuring reliable isotope abundance data. This transmission is ensured for a field of view of ± 5° with respect to ram (flight) direction.

3. Electronics

The electronics relies on a mixed board design, as usual for such types of instruments. A detailed description of necessary subsystems for space-borne mass spectrometers is provided in reference [23]. The electronics of the CubeSatTOF represents a slight adaptation to previously used systems [23], [24] given the opportunity of using commercial off-the-shelf (COTS) components in CubeSat-type projects.

The electronics of the CubeSatTOF is accommodated on 5 printed circuit boards (PCBs, Figure 1). Four of them are stacked forming a card rack and the detector board is mounted orthogonally to the sensor board (see Figure 2). The placement of electronic subsystems in a 1 U cube considerably influences the scientific performance and engineering effort that is necessary for the development of the instrument. On one hand, all relevant subsystems are in close proximity to its consumer. This is especially relevant for high voltage power supplies and high-speed electronics such as the detector and its supporting electronics. On the other hand, noise-sensitive subsystems such as, for example, the detector with related electronic front-end benefit from a decoupling from noise sources, such as, for example, the high

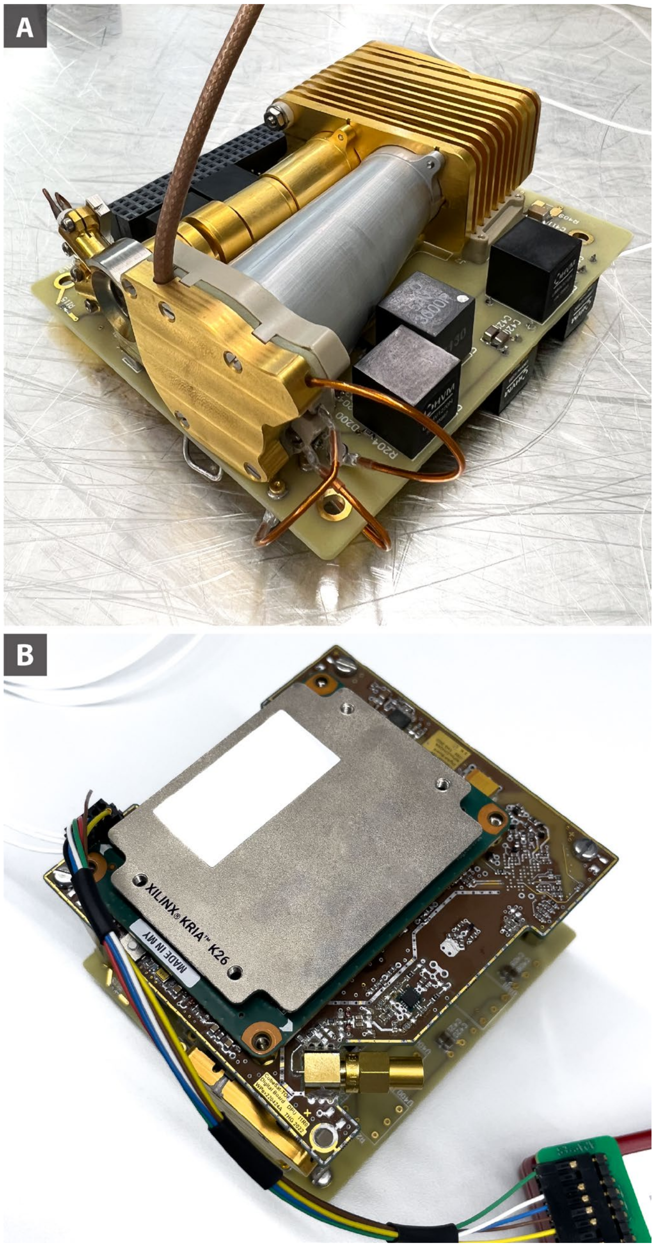

Figure 2. Sensor board (A) with digital board on top of it (B), both at prototype level.

voltage pulser. The mixed board design results in a highly integrated instrument.

Sensor board

The *sensor board* supports the ion-optical system, which is mounted on the PCB. The electrodes comprising the ion-optical system are directly connected to the PCB circuit through the screws fixing those electrodes in place. We decided to place the high voltage power supplies (HVPS) on this PCB as well. Hence, as compared to previous instruments, bulky high voltage connectors and stiff harnesses are not necessary. This architecture reduces risks, shortens both development time and budget, and allows for a considerable miniaturization.

Mostly, COTS components are used for the HVPS. CubeSatTOF relies on seven HVPS, of which one has a minimum voltage of nominally –1800 V, two –900 V, and three below +400 V. Another power supply floats on the detector bias voltage. They are controlled with an analogue 0 to 5 V input voltage each and connected via the serial peripheral interface (SPI bus) to the data processing unit (DPU).

An additional subsystem that benefits from omitting the transmission line is the high voltage pulser. The high voltage pulser rises from about 0 V to nominally +220 V with a rise time of about 2 ns. The high voltage pulse is created on the opposite side of the ion source on the PCB, i.e., directly at the location where it is needed. Thus, the pulse rise time benefits from the reduced capacitance of the omitted transmission line. This low pulse rise time is mainly responsible for the instrument's high mass resolution, especially at low *m/z*. The pulser is connected either to its drivers on the *digital board* or to an external breadboard for commissioning.

Using fast high voltage pulsers usually creates a noisy electronic environment contrasting single ion measurement. Therefore, the *detector board* is mounted on the second drift tube of the ion-optical system. This PCB also supports the MCP chevron stack, the anode collecting the electrons created by the MCPs, and limited detector proximity electronics. Most supporting electronics, i.e., filters and power supplies, are placed on the *sensor board* to save space on the *detector board.* We found that the sensitivity of the measurements would benefit only moderately from a decoupling of the pulser structure. Hence, the developed detector is compact and it can easily be shielded from particle radiation if desired (which is likely not the case for the initial versions of the flight instrument to be placed in LEO). Three cables connect the proximity electronics to the *sensor board* by simple, robust M1.6 cable lugs. This allows for sufficient mating cycles, even during commissioning phase and saves space as well. Thus, the sensitive components of the detector are actually decoupled from the *sensor board*. A 50 Ω terminated coaxial cable transmits the signal from the anode to the *digital board*. Here, we decided to rely on an SMA connector to simplify debugging with an oscilloscope. There is space for this SMA connector. Hence, the flight design will incorporate this connector as well, accelerating the commissioning phase.

Digital board

The *digital board* incorporates two subunits namely the carrier board and the DPU. The carrier board includes the following subsystems: front-end electronics with high-speed analog-to-digital converter (ADC) for signal acquisition, modules for housekeeping (HK), and modules for communication with both the spacecraft and the electronic ground support equipment (EGSE).

DPU with SOM and FPGA—The DPU with its field-programmable gate arrays (FPGA) is located on a system on module (SOM). For simplicity, we later refer to this package as DPU. To prove the concept of miniaturization, we selected *Xilinx, Inc.*'s Kria K26 as SOM, on which the FPGA is located and hence the DPU operates. Besides the existing libraries for digital data processing, programmable software (PS), and programmable logic (PL), its power saving capability is beneficial for this application, as unused features can be switched off. An ultra-compact board-to-board connector connects the carrier board and the SOM and an additional connector provides connection to the other boards to read out HK via an SPI bus.

The DPU collects data, processes them, and forwards them to other subsystems. Figure 4 provides an overview of these data flows in the digital design and their physical location on the *digital board*. On the input side, the SOM reads out HK data to monitor the status of the *digital board*, in addition to the locally generated HK data that are fetched via SPI bus. Also, the analog signal processing with its high-speed ADC and front-end inputs the SOM. The SOM provides an internal file system, programmable software and programmable logic. On the output side, transmission modules (PHY and TRANS) enable communication and digital-to-analog converters (DAC) allow for controlling the periphery.

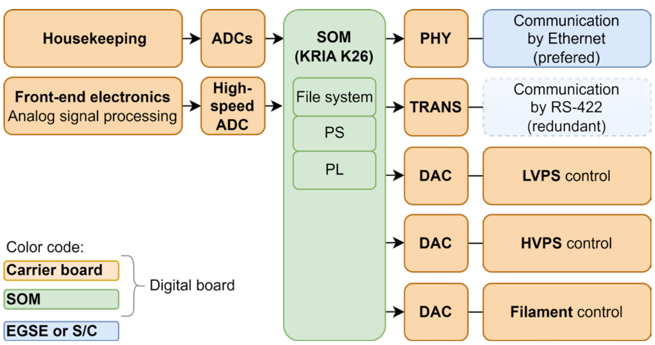

Figure 4. Location of the subsystems on the *digital board*.

A DPU-internal file system holds information on the current configuration of the instrument (Figure 5). Modifying this configuration file will cause updates to the instrument's parameters. For example, to change the emission current of the cathode, or to adapt the voltages applied to the electrodes, this file, referred to as the MeasConfig file, has to be adapted. Even the commands for initializing measurements are mapped through this parameter file. Once the update is recognized, the system allows for some settling time before triggering the pulser (see also Figure 3). A second triggering system for either technological use or for blanking selected species preventing the detector from saturation is anticipated, but not used in the current configuration of the instrument. In parallel, the set values on the periphery are updated. If a measurement process is started, then the acquisition process is initiated and the resulting data files are stored in the Meas IDx files.

Time-of-flight mass spectrometers react sensitive to both jitter in the analog domain and different response times in the digitized signal path. Deviations have a direct impact on the measurement quality. Histogramming of spectra is performed

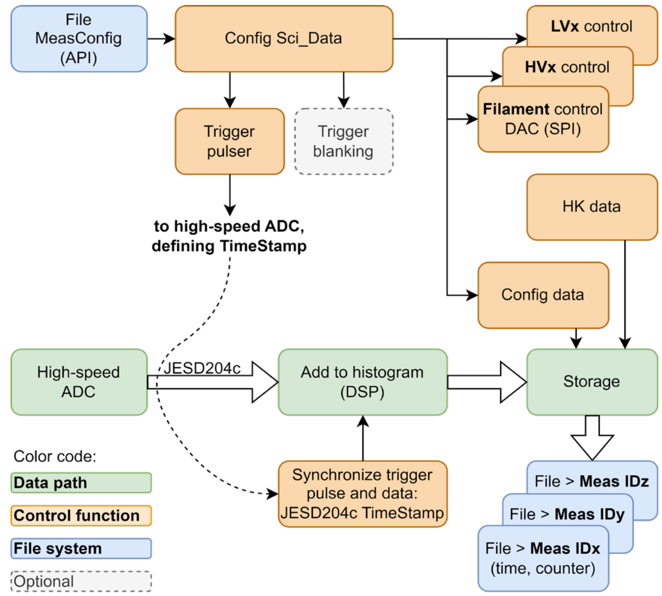

Figure 5. The process from initiating a measurement by modification of the MeasConfig file to the final data is shown.

to improve the signal to noise ratio by about a factor of the square root of the number of accumulated waveforms. If there is jitter, then the Gaussian peak of a mass line in the final spectrum is broadened correspondingly, reducing the mass resolution and the signal to noise ratio. Thus, we focused on minimizing jitter and other time relevant distortion between the DPU and the ADC.

The CubeSatTOF instrument implements a dedicated triggering system and related architecture ensuring low jitter measurements (Figure 3). Once a measurement is scheduled, the DPU on the SOM writes a timestamp into a register of the high-speed ADC register. The ADC outputs a (5V) transistor-transistor logic (TTL) signal triggering the high voltage pulser of the ion-optical system. In parallel, the modification in the register interrupts the ADC triggering the digitization of the analog ADC input signal. The JESD204c data packages (standardized serial interface) include this timestamp as a marker. The DPU monitors these timestamps in the ADC data readout stream. Once a relevant timestamp is detected in the stream, it distributes the integers of the waveform to histogram the signal, as on board digital signal processing (DSP). This process is repeated until the desired number of waveforms are accumulated (the integration time).

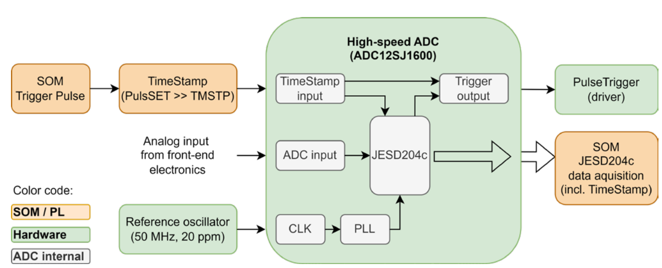

Figure 3. Triggering system of the CubeSatTOF instrument.

The DPU stores the spectrum in a data file once the accumulation process has finished.

Given this concept, the accuracy of the timestamp is crucial. Therefore, an accurate external local oscillator clocks the ADC ensuring phase jitter in the low femtosecond range. Given this low jitter of the clock and as all time-critical processes are performed inside the ADC based on the internal phase-locked loop (PLL), the dominating source of the jitter affecting the sampling is the ADC itself, which has a typical jitter time of 0.71 ns according to the specification [25].

Front-end with high-speed ADC—The SMA connector inputs the raw analog signal of the *detector board* into the analog electronics front-end. A protection and input filter circuit protects the front-end from overcurrent. Two gain stages amplify the signal. A third order low pass filter at a cut-off frequency of about 800 MHz prevents aliasing before digitization with a 12-bit high-speed ADC supplied by *Texas Instruments*, *Inc.* (ADC12SJ1600; 9.0 ENOB at 800 MHz) operating at 1.6 GHz. This high-end ADC delivers the sampled data through a state of the art JESD204c interface to the DPU for further digital data processing.

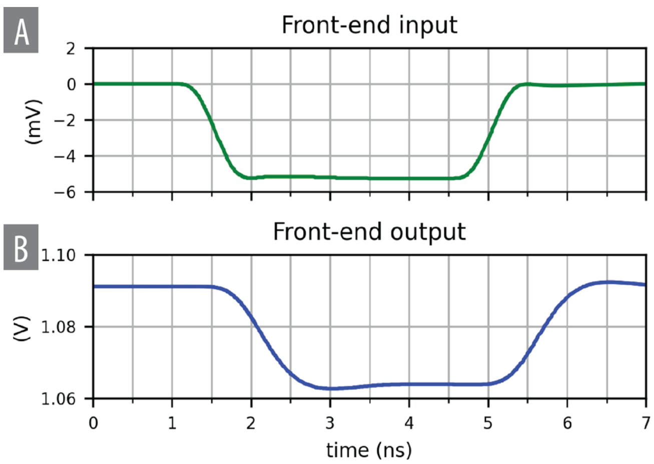

Figure 6. Estimated detector output that corresponds to the input of the electronic front-end (green, A) and the front-end output (blue, B).

As necessary for recording signals in the time domain, the front-end electronics benefit from minimizing the frequency-dependent phase shift over the used frequencies. Figure 6 shows the simulation of the transfer function of the front-end in the time domain. For this simulation performed in LTspice from Linear Technology, Inc., the input signal is modeled with a pulse of 5 mV in 3 ns (Figure 6, panel A). The front-end provides a gain of about 5 (Figure 6, panel B), which is sufficient for sampling with the ADC, in analogy to previously developed electronic front-ends (for example, reference [23]).

Figure 7 presents the performance of the front-end electronics in a Bode plot. Panel A shows the classical Bode plot with the solid line representing the gain (left-hand scale) and the dotted line representing the phase (right-hand scale). Panel B

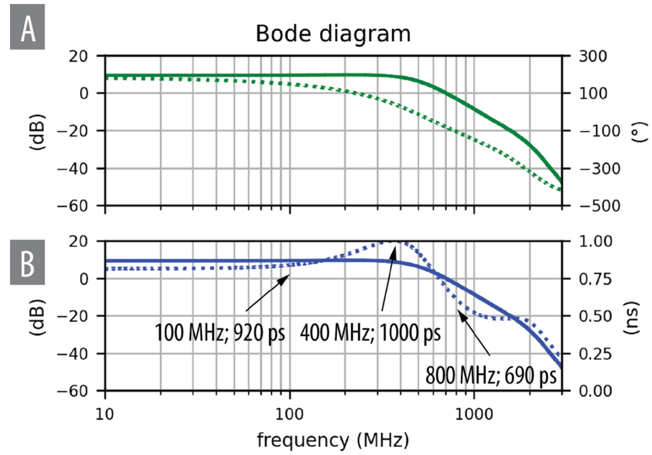

Figure 7. Bode diagram of the front-end. A description is provided in the text.

shows the gain for reference (solid line) and the individual time delays (dotted line). This LTspice simulation shows an expected maximal runtime difference of about 310 ps at 800 MHz. Even though this runtime difference results in some distortion of the signal, its impact is negligible, hence the front-end electronics maintain a constant group delay in a sufficiently accurate manner.

Communication interfaces—The digital board hosts communication interfaces for inter-board communication, i.e., the SPI bus and output of drivers, and dedicated interfaces for communication with either the EGSE or the spacecraft. Experience has shown that the commissioning phase is considerably accelerated if including a high-speed communication interface. Therefore, we implemented Ethernet in addition to the usually implemented RS-422 interface. A universal asynchronous receiver transmitter (UART) console allows for direct communication with the DPU for debugging.

During commissioning and development, the DPU hosts a hypertext transfer protocol (HTTP) server that provides an application programming interface (API) with standard HTTP request methods such as DELETE, GET, PATCH, POST, and PUT to operate it as an internet-of-things (IOT) device. This web server provides easy access to control the status of the instrument by updating the internal MeasConfig files. The typical output data package includes housekeeping of the instrument in the header and scientific data in the payload of a data product.

Power Board

First, the power for consumers is prepared on the *power board*. The EGSE or the spacecraft inputs 12 V direct current (DC). An additional circuitry for filtering and current limiting protects the instrument. The stabilized voltage is either distributed directly, or converted to +5V and +3.3V via DC/DC converters to provide input voltages for the consumers. Second, in contrast to the high voltages, low voltage can easily be transported from one board to another. Thus, we placed the low voltage power supplies (LVPS) on

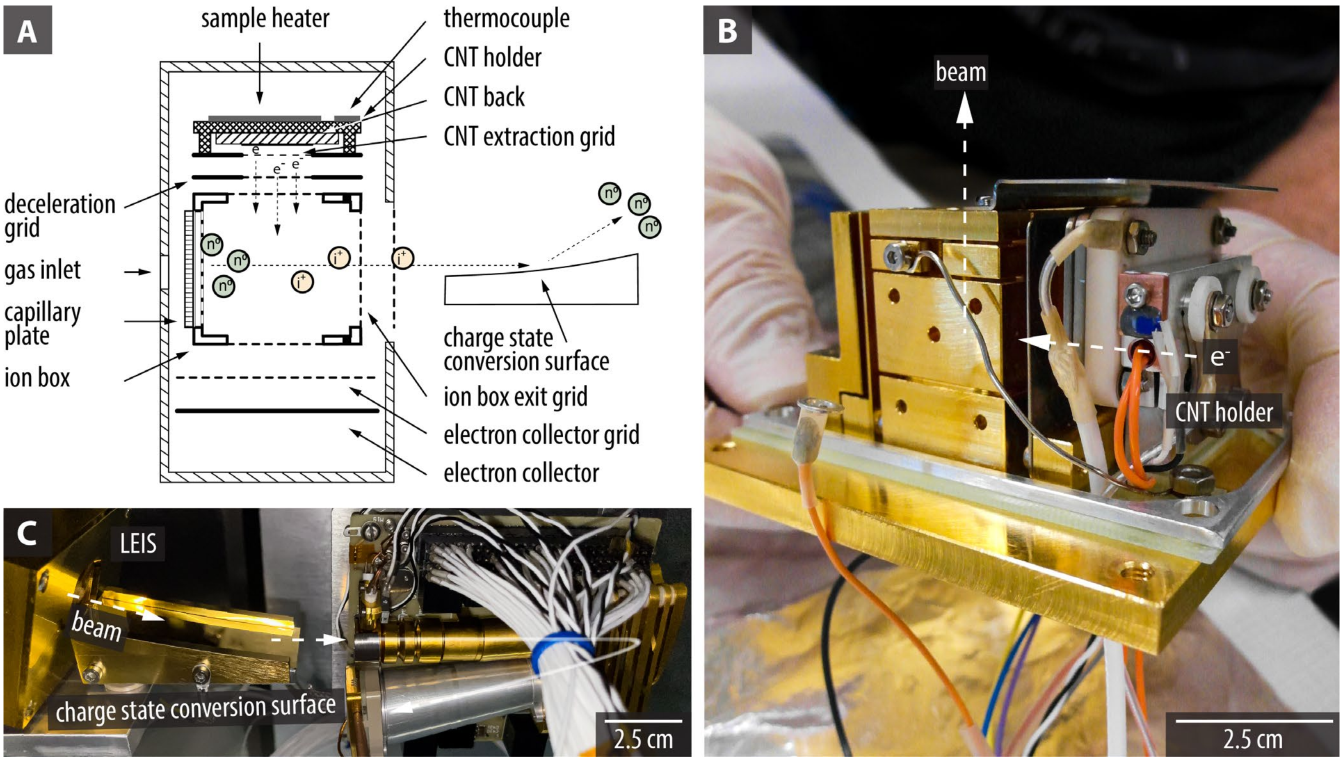

Figure 8. Schematics (A; not to scale) and hardware (C) of the LEIS with charge state conversion surface. The interior shows the mounting of the CNT related setup (B). The text describes abbreviations.

this board and connected them to the *sensor board* with the board-to-board connector. The ion-optical system requires two variable LVPS providing ±12 V and three providing –100 V. Third, the filament controller is located on the *power board*. The baseline for heating the filament is a low power consumption, alternating current (AC) driver [23]. As this driver creates some noise, we placed it far away from the ion-optical system and the read-out electronics. In fact, insusceptible locations on the *digital board* are used for shielding the ion-optical system from noise. Fourth, we reserved space on this board to anticipate a driver that is used on the *technology board*.

Technology Board

On one hand, the philosophy of CubeSatTOF is to provide a robust instrument at very low risks to ensure a high probability of failure-free operation despite accepting COTS components. On the other hand, CubeSatTOF includes some redundant subsystems for technology demonstration in space, to gain technical readiness level (TRL) 9. Although the evaluation process of technologies to be tested is ongoing, we favor testing COTS HVPS and subsystems of a tunable laser system for selective ionization of species. The technology board will be populated with devices under testing (DUTs) in accordance with the needs for other, future mass spectrometers on major spacecraft (see reference [20], for example).

4. TEST FACILITIES

Providing a beam of neutral species at orbital velocities is a major challenge. Currently available facilities offer the capability to accelerate neutrals up to 4.2 km/s for H, and considerably lower for heavier masses, i.e., in the order of km/s [13], [24], [26]. Hence, we modified a low energy ion source (LEIS) [27]. It was originally designed to generate low energetic ions with energies in the range of 1 to 20 eV with which the mass spectrometers on board ROSINA / ROSETTA were calibrated. This was necessary, as thermionic emitters heated the gas too much, being unrepresentative for the cold exosphere of the comet 67P / Churyumov-Gerasimenko [27]. We upgraded LEIS to anticipate ions and neutral particles with energies up to 2 keV. This allows for calibration of mass spectrometers performing hypervelocity flybys or experience orbital velocity in LEO, as do NIM on board JUICE [24] and this instrument [11]. Given the schedules of both instruments, LEIS is expected to be fully operational in spring 2023.

Figure 8, panel A shows a schema of LEIS with a charge state conversion surface attached to illustrate the working principle. The test gas penetrates the ion box of LEIS through a plate consisting of many capillaries. By flowing through the capillaries, the gas is directed towards the exit of the ion box.

During this flow, electron ionization ionizes the gas. Carbon nanotubes (CNTs) are used to generate the electron beam orthogonal to the gas flow direction [28] (Figure 8, panel B). CNTs are field emitters. Thus, the electrons are extracted from the CNTs by applying a high voltage of about 2 kV on a grid in front of the CNTs. The advantages of using CNTs compared to hot cathodes are that they only add a narrow additional energy distribution to the energy of the generated ion beam, as the system remains at about room temperature. In addition, they consume much less power and have a bigger surface from which they emit electrons to ionize the whole volume of the ion box. The CNTs in LEIS can be heated up to 100°C to accelerate outgassing. The electron collector opposite of the CNTs measures the current established by the electrons reaching the opposite side of the ion box indicating the status of ionization.

Once the species are ionized inside the ion box, they are accelerated by the electrostatic fields, i.e., the voltage difference between the ion box and the outer cover of LEIS. This potential difference corresponds to the energy of the ions. LEIS can be floated to voltages between ±20 V to simulate spacecraft charging effects.

To generate a beam consisting of neutral particles out of the ion beam, a charge state conversion surface has been attached to the LEIS (Figure 8, panels A and C). The ions graze the conversion surface and pick up an electron. In this process, they lose about 11 to 15 % of their initial energy [29] and the ionization efficiency is about 80 % empowered by the gold-coated silicon wafer as a charge state conversion surface.

5. CONCLUSION

Monitoring space weather requires in situ measurements with sensitive mass spectrometers. We developed a CubeSat-type time-of-flight mass spectrometer that fits into 1 U and provides a scientific performance to be applied to use in the upper atmosphere. We showed that a miniaturization is possible while maintaining the relevant scientific performance. The anticipated performance in space flight in conjunction with the CHESS mission supplies the community with desperately needed chemical composition and neutral density data of the upper atmosphere, in almost real-time.

LIST OF ABBREVIATIONS, ACRONYMS AND SYMBOLS

AC	Alternating Current
ADC	Analogue to Digital Converter
API	Application Programming Interface
BB	Breadboard
CHESS	Constellation of High-Performance Exosphere Science Satellites
CNT	Carbon Nanotube
COTS	Commercial Off-The-Shelf
CubeSatTOF	CubeSat Time-Of-Flight mass spectrometer
DAC	Digital to Analog Converter
DC	Direct Current
DPU	Data Processing Unit
DSP	Digital Signal Processing
DUT	Device Under Testing
DYNAMIC	Dynamical Neutral Atmosphere-Ionosphere Coupling
EGSE	Electronic Ground Support Equipment
ENOB	Effective Number Of Bits
ESA	European Space Agency
FPGA	Field-Programmable Gate Array
FWHM	Full Width at Half Maximum
GNSS	Global Navigation Satellite System
HK	Housekeeping
HTTP	Hypertext Transfer Protocol
HVPS	High voltage power supply
IOS	Ion-Optical System
IOT	Internet Of Things
JUICE	JUpiter ICy moon Explorer
LEIS	Low Energy Ion Source
LEO	Low Earth Orbit
LVPS	Low Voltage Power Supply
m	Mass
m/z	Mass per charge ratio
m/Δm	Mass resolution
Δm	Peak width of mass of interest, measured as FWHM
MCP	Multi-Channel Plate
NASA	National Aeronautics and Space Administration
NGMS	Neutral Gas Mass Spectrometer
NIM	Neutral and Ion Mass spectrometer
PCB	Printed Circuit Board
PLL	Phase-Locked Loop
PEP	Particle Exploration Package
PL	Programmable Logic
PS	Programmable Software
R	Mass resolution
ROSINA	Rosetta Orbiter Spectrometer for Ion and Neutral Analysis
SOM	System On a Module
SPI	Serial Peripheral Interface
TOF	Time-Of-Flight
TRL	Technical Readiness Level
TTL	Transistor-Transistor Logic
U	Unit (measure for the volume of a CubeSat)
UART	Universal Asynchronous Receiver Transmitter

ACKNOWLEDGEMENTS

The mechanical and electronics engineering team of the Physics Institute of the University of Bern is acknowledged. We thank Michael Pichler from the University of Applied Sciences and Arts Northwestern Switzerland (FHNW) for his consultancy regarding the FPGA design.

REFERENCES

[1] R. A. Vincent, "The dynamics of the mesosphere and lower thermosphere: a brief review," *Prog. Earth Planet. Sci.*, vol. 2, no. 1, p. 4, Mar. 2015, https://doi.org/10.1186/s40645-015-0035-8.

[2] J. Laštovička, "Trends in the upper atmosphere and ionosphere: Recent progress," *J. Geophys. Res. Sp. Phys.*, vol. 118, no. 6, pp. 3924–3935, Jun. 2013, https://doi.org/10.1002/jgra.50341.

[3] J. Laštovička, G. Beig, and D. R. Marsh, "Response of the mesosphere-thermosphere-ionosphere system to global change - CAWSES-II contribution," *Prog. Earth Planet. Sci.*, vol. 1, no. 1, p. 21, Dec. 2014, https://doi.org/10.1186/s40645-014-0021-6.

[4] M. Palmroth *et al.*, "Lower-thermosphere–ionosphere (LTI) quantities: current status of measuring techniques and models," *Ann. Geophys.*, vol. 39, no. 1, pp. 189–237, Feb. 2021, https://doi.org/10.5194/angeo-39-189-2021.

[5] T. E. Sarris, "Understanding the ionosphere thermosphere response to solar and magnetospheric drivers: status, challenges and open issues," *Philos. Trans. R. Soc. A Math. Phys. Eng. Sci.*, vol. 377, no. 2148, p. 20180101, Jul. 2019, https://doi.org/10.1098/rsta.2018.0101.

[6] R. A. Hoffman, "Dynamics Explorer Program," *Eos, Trans. Am. Geophys. Union*, vol. 61, no. 44, pp. 689–692, 1980, https://doi.org/10.1029/EO061i044p00689.

[7] National Research Council, *Solar and Space Physics*. Washington, D.C.: National Academies Press, 2013. https://doi.org/10.17226/13060.

[8] T. J. Fuller-Rowell, "The Dynamics of the Lower Thermosphere," in *The Upper Mesosphere and Lower Thermosphere: A Review of Experiment and Theory, Volume 87*, R. M. Johnson and T. L. Killeen, Eds. American Geophysical Union, 2013, pp. 23–36. https://doi.org/10.1029/GM087p0023.

[9] J. T. Emmert, "Thermospheric mass density: A review," *Adv. Sp. Res.*, vol. 56, no. 5, pp. 773–824, Sep. 2015, https://doi.org/10.1016/j.asr.2015.05.038.

[10] R. A. Akmaev, "Whole atmosphere modeling: Connecting terrestrial and space weather," *Rev. Geophys.*, vol. 49, no. 4, 2011, https://doi.org/10.1029/2011RG000364.

[11] R. G. Fausch, G. Moeller, M. Rothacher, N. Martinod, T. Trebaol, A. Villegas, J.-P. Kneib, F. Corthay, M. Joss, F. Tieche, M. Tulej, and P. Wurz, "CHESS: Measuring the Dynamics of Composition and Density of Earth's Upper Atmosphere with CubeSats," *2022 IEEE Aerosp. Conf.*, pp. 01–13, Mar. 2022, https://doi.org/10.1109/AERO53065.2022.9843791.

[12] W. C. Wiley and I. H. McLaren, "Time-of-Flight Mass Spectrometer with Improved Resolution," *Rev. Sci. Instrum.*, vol. 26, no. 12, pp. 1150–1157, Dec. 1955, https://doi.org/10.1063/1.1715212.

[13] R. G. Fausch, P. Wurz, B. Cotting, U. Rohner, and M. Tulej, "Direct Measurement of Neutral Gas during Hypervelocity Planetary Flybys," *2022 IEEE Aerosp. Conf.*, pp. 1–12, Mar. 2022, https://doi.org/10.1109/AERO53065.2022.9843767.

[14] R. Fausch, P. Wurz, U. Rohner, and M. Tulej, "CubeSatTOF: Planetary Atmospheres Analyzed with a 1U High-Performance Time-Of-Flight Mass Spectrometer," in *Proceedings of the 34th Small Satellite Conference*, 2020, no. SSC20-WKII-02, pp. 1–10. [Online]. Available: https://digitalcommons.usu.edu/smallsat/2020/all2020/14/

[15] W. E. Wallace, "Mass Spectra," in *NIST Chemistry WebBook, NIST Standard Reference Database Number 69*, 2022. https://doi.org/https://doi.org/10.18434/T4D303.

[16] B. Mamyrin, V. Karataev, D. Shmikk, and V. Zagulin, "The mass-reflectron, a new nonmagnetic time-of-flight mass spectrometer with high resolution," *Sov. J. Exp. Theor. Phys.*, vol. 37, no. 1, p. 45, 1973.

[17] S. Scherer, K. Altwegg, H. Balsiger, J. Fischer, A. Jäckel, A. Korth, M. Mildner, D. Piazza, H. Reme, and P. Wurz, "A novel principle for an ion mirror design in time-of-flight mass spectrometry," *Int. J. Mass Spectrom.*, vol. 251, no. 1, pp. 73–81, Mar. 2006, https://doi.org/10.1016/j.ijms.2006.01.025.

[18] P. Wurz and L. Gubler, "Impedance-matching anode for fast timing signals," *Rev. Sci. Instrum.*, vol. 65, no. 4, pp. 871–876, 1994, https://doi.org/10.1063/1.1144914.

[19] L. Hofer, P. Wurz, A. Buch, M. Cabane, P. Coll, D. Coscia, M. Gerasimov, D. Lasi, A. Sapgir, C. Szopa, and M. Tulej, "Prototype of the gas chromatograph–mass spectrometer to investigate volatile species in the lunar soil for the Luna-Resurs mission," *Planet. Space Sci.*, vol. 111, no. 1, pp. 126–133, Jun. 2015, https://doi.org/10.1016/j.pss.2015.03.027.

[20] R. G. Fausch, J. A. Schertenleib, and P. Wurz, "Advances in Mass Spectrometers for Flyby Space Missions for the Analysis of Biosignatures and Other Complex Molecules," *Universe*, vol. 8, no. 8, p. 416, Aug. 2022, https://doi.org/10.3390/universe8080416.

[21] J. Klenzing, R. L. Davidson, S. L. Jones, C. Martinis, K. A. Zawdie, G. D. Earle, J. M. Smith, A. J. Halford, S. Noel, N. Paschalidis, R. F. Pfaff, and E. Robertson, "The petitSat mission – Science goals and instrumentation," *Adv. Sp. Res.*, vol. 66, no. 1, pp. 107–115, Jul. 2020, https://doi.org/10.1016/j.asr.2019.12.013.

[22] T. E. Sarris *et al.*, "Daedalus: a low-flying spacecraft for in situ exploration of the lower thermosphere–ionosphere," *Geosci. Instrumentation, Methods Data Syst.*, vol. 9, no. 1, pp. 153–191, Apr. 2020, https://doi.org/10.5194/gi-9-153-2020.

[23] R. G. Fausch, P. Wurz, M. Tulej, J. Jost, P. Gubler, M. Gruber, D. Lasi, C. Zimmermann, and T. Gerber, "Flight electronics of GC-mass spectrometer for investigation of volatiles in the lunar regolith," *2018 IEEE Aerosp. Conf.*, pp. 1–13, 2018, https://doi.org/10.1109/AERO.2018.8396788.

[24] M. Föhn, A. Galli, A. Vorburger, M. Tulej, D. Lasi, A. Riedo, R. G. Fausch, M. Althaus, S. Brungger, P. Fahrer, M. Gerber, M. Luthi, H. P. Munz, S. Oeschger, D. Piazza, and P. Wurz, "Description of the Mass Spectrometer for the Jupiter Icy Moons Explorer Mission," in *2021 IEEE Aerospace Conference*, Mar. 2021, pp. 1–14. https://doi.org/10.1109/AERO50100.2021.9438344.

[25] TI, "ADC12xJ1600-Q1 Quad/Dual/Single Channel, 1.6-GSPS, 12-bit, Analog-to-Digital Converter (ADC) with JESD204C Interface," Datasheet, Texas Instruments Incorporated, 2020.

[26] S. Graf, K. Altwegg, H. Balsiger, A. Jäckel, E. Kopp, U. Langer, W. Luithardt, C. Westermann, and P. Wurz, "A cometary neutral gas simulator for gas dynamic sensor and mass spectrometer calibration," *J. Geophys. Res. E Planets*, vol. 109, no. 7, p. E07S08, 2004, https://doi.org/10.1029/2003JE002188.

[27] M. Rubin, K. Altwegg, A. Jäckel, and H. Balsiger, "Development of a low energy ion source for ROSINA ion mode calibration," *Rev. Sci. Instrum.*, vol. 77, no. 10, p. 103302, Oct. 2006, https://doi.org/10.1063/1.2358708.

[28] H. Zhang, D. Li, P. Wurz, A. Etter, Y. Cheng, C. Dong, and W. Huang, "Performance of a low energy ion source with carbon nanotube electron emitters under the influence of various operating gases," *Nanomaterials*, vol. 10, no. 2, 2020, https://doi.org/10.3390/nano10020354.

[29] M. Wieser and P. Wurz, "Production of a 10 eV–1000 eV neutral particle beam using surface neutralization," *Meas. Sci. Technol.*, vol. 16, no. 12, pp. 2511–2516, Dec. 2005, https://doi.org/10.1088/0957-0233/16/12/016.

BIOGRAPHY

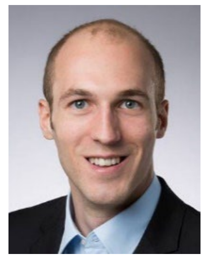

Rico Fausch *completed an apprenticeship as a mechanical design engineer before he received a B.Sc. in Systems Engineering (micro technologies) from NTB University of Applied Science (Switzerland) in 2013 and an M.Sc. in Biomedical Engineering from University of Bern (Switzerland) in 2015. He has been with the Physics Institute of the University of Bern since 2016, where he received his Ph.D. in Physics in 2020 for the finalization of the NGMS/Luna-Resurs. As a post-doctoral researcher, he is involved in the design of several space missions and space instrumentation including NIM/JUICE.*

Claudio Zimmermann *received a M.Sc. in Electrical Engineering from the federal institute of Technology Lausanne (1998, Switzerland). In its own company, he gained large experience in building Laser machines for micromachining and developing electronic hardware for Aircraft Engine Control Units. Starting in 2013 at the University of Bern (Switzerland), he designed and qualified the electronic hardware for the Colour and Stereo Surface Imaging System (CaSSIS) on board the TGO satellite of the ESA ExoMars mission. He is involved in the development of the CubeSatTOF electronics. In the new formed Detector Lab, he designed and built space-like electronics for commanding and reading out CMOS image detectors. Currently, he develops electronics for the comet camera (CoCa) on the Comet Interceptor mission from ESA.*

Thomas Gerber *received a B.Sc. in Electronics Information and Communication Technologies (ICT) from the Bern University of Applied Sciences (Switzerland) in 2012. He has been with the University of Bern since 2015, where he has worked as electrical engineer for the CASSIS camera on board ESA's ExoMars mission and the neutral gas mass spectrometer (NGMS) on board the joint ESA-Roscosmos Luna-Resurs mission. Currently, he develops electronics for the comet mass spectrometer and neutral density gauge (MANIaC) on ESA's Comet Interceptor mission. Within the scope of his master thesis, he is* *involved in the development of the CubeSatTOF instrument for the CHESS mission.*

Janis Schertenleib *obtained his Bachelor's degree in Physics from the University of Bern (Switzerland) in 2021. He is currently pursuing a Master's degree in Experimental Physics, also at the University of Bern. For his master thesis, he is working at the Space Science and Planetology division, designing and testing ion optical systems for time-of-flight mass spectrometers. He is also involved in the CHESS space mission, a collaboration between the University of Bern, the École Polytechnique Fédérale in Lausanne (EPFL) and the Eidgenössische Technische Hochschule Zürich (ETHZ).*

Martina Föhn *received an M.Sc. in physics from the University of Bern (Switzerland) in 2017, with a thesis on the scattering properties of charge state conversion surfaces for space applications for the JUICE and the IMAP missions. She received her PhD in 2021 for the development of the NIM insrument on board JUICE and has been involved in many space missions since then.*

Audrey Aebi *has been studying for a Bachelor's degree in physics at the University of Bern (Switzerland) since 2020. In the student council, she is active as an event organizer. In addition to her work as an observer at the Zimmerwald Observatory (Switzerland), she completed an internship at the Space Science and Planetology division Department of Space Research and Planetology at the University of Bern, where she was involved in the development of the CubeSatTOF instrument.*

Peter Wurz *has a degree in electronic engineering (1985), an M.Sc. and a Ph.D. in Physics from Technical University of Vienna (1990). He has been a post-doctoral researcher at Argonne National Laboratory. At the University of Bern since 1992, he is a professor of physics and since 2015 head of the Space Science and Planetology division. He has been Co-I and PI for many science instruments for space missions of ESA, NASA, ISRO, Roscosmos, and JAXA. He is PI of NIM and Co-PI of PEP on board JUICE.*